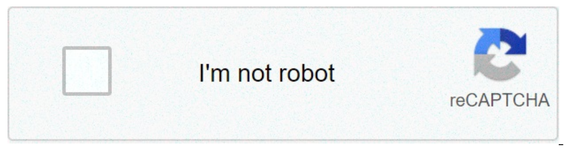

Continue

How to find molar enthalpy change

Molar Heat of Combustion: The heat liberated when one mole of a certain compound undergoes complete combustion with oxygen at a constant pressure of exactly one atmosphere (100 kPa) and at 25°C with the final products being carbon dioxide gas and liquid water. Heats of combustion are quoted as positive numbers while the enthalpy changes of combustion reactions (ΔH) are quoted as negative numbers, as combustion reactions are always exothermic. Heats of combustion are typically stated in kilojoules per mole (kJ/mol. or kJ mol.-1). The accepted value for the molar heat of combustion of ethanol is 1360 kJ mol.-1. The following steps allow the calculation of an experimental value for the molar heat of combustion of ethanol: Measure and record the mass of a burner containing ethanol. Measure 100 mL of water into a beaker and measure the temperature of the water. Place the beaker of water directly above the burner and light it. Allow the burner to heat the water for one minute, then extinguish it. Immediately measure and record the mass of the burner and the temperature of the water. Calculate the change in mass and the change in temperature. Substitute the experimental results into the formula below to determine the enthalpy change: where: ΔH = enthalpy change in joules m = mass of water C = thermal capacity (4.2 for water) ΔT = change in temperature in degrees Celsius Determine the number of moles of ethanol combusted (number of moles = mass/FM), and divide the enthalpy change in kilojoules by this number to determine the experimental value of the molar heat of combustion of ethanol in kilojoules per mole. Due to heat loss to surroundings, the experimental value of the molar heat of combustion of ethanol will be significantly lower than the accepted value. If the same experiment was conducted for another alkanol, such as methanol, and the difference between the experimental value and accepted value was found, this difference could be used to calibrate the experimental results for ethanol and produce a more accurate experimental result. The process described above can be applied to any alkanol, and can be modified slightly in order to find the heat of combustion in kilojoules per gram instead of kilojoules per mole. report this ad You use the standard enthalpy of the reaction and the enthalpies of formation of everything else. For most chemistry problems involving #ΔH_f^o#, you need the following equation: #ΔH_(reaction)^o = ΣΔH_f^o(p) - ΣΔH_f^o(r)#, where p = products and r = reactants. EXAMPLE: The #ΔH_(reaction)^o# for the oxidation of ammonia $4NH_3(g) + 5O_2(g) \rightarrow 4NO(g) + 6H_2O(g)$ is -905.2 kJ. Calculate #ΔH_f^o# for ammonia. The standard enthalpies of formation are: NO(g) = +90.3 kJ/mol and $H_2O(g)$ = -241.8 kJ/mol. Solution: $4NH_3(g) + 5O_2(g) \rightarrow 4NO(g) + 6H_2O(g)$ #ΔH_(reaction)^o = ΣΔH_f^o(p) - ΣΔH_f^o(r)# #ΣΔH_f^o(p) = 4 mol NO×(+90.3 kJ)/(1 mol NO) + 6 mol H_2O×(-241.8 kJ)/(1 mol H_2O)# = 361.2 kJ – 1450.8 kJ = -1089.6 kJ #ΣΔH_f^o(r) = 4 mol NH_3 × (x kJ)/(1 mol NH_3) + 5 mol O_2 × (0 kJ)/(1 mol O_2)# = 4x kJ #ΔH_(reaction)^o = ΣΔH_f^o(p) - ΣΔH_f^o(r)#; so -905.2 kJ = -1089.6 kJ – 4x kJ 4x = -184.4 x = -46.1 #ΔH_f^o#(NH_3) = x kJ/mol = -46.1 kJ/mol If you're seeing this message, it means we're having trouble loading external resources on our website. If you're behind a web filter, please make sure that the domains *.kastatic.org and *.kasandbox.org are unblocked. Something went wrong. Wait a moment and try again. Something went wrong. Wait a moment and try again. Calculations: Molar Enthalpysamabrhms112019-06-02T23:21:48+01:00 Oxygen migration enthalpy likely limits oxide precipitate dissolution during tabula rasa SciTech Connect Looney, E. E.; Laine, H. S.; Youssef, A. In industrial silicon solar cells, oxygen-related defects lower device efficiencies by up to 20% (rel.). In order to mitigate these defects, a high-temperature homogenization anneal called tabula rasa (TR) that has been used in the electronics industry is now proposed for use in solar-grade wafers. This work addresses the kinetics of tabula rasa by elucidating the activation energy governing oxide precipitate dissolution, which is found to be 2.6 +/- 0.5 eV. This value is consistent within uncertainty to the migration enthalpy of oxygen interstitials in silicon, implying TR to be kinetically limited by oxygen point-defect diffusion. This large activation energymore » is observed to limit oxygen precipitate dissolution during standard TR conditions, suggesting that more aggressive annealing conditions than conventionally used are required for complete bulk microdefect mitigation.« less Enhancing Entropy and Enthalpy Fluctuations to Drive Crystallization in Atomistic Simulations. PubMed Piaggi, Pablo M; Valsson, Omar; Parrinello, Michele 2017-07-07 Crystallization is a process of great practical relevance in which rare but crucial fluctuations lead to the formation of a solid phase starting from the liquid. As in all first order first transitions, there is an interplay between enthalpy and entropy. Based on this idea, in order to drive crystallization in molecular simulations, we introduce two collective variables, one enthalpic and the other entropic. Defined in this way, these collective variables do not prejudge the structure into which the system is going to crystallize. We show the usefulness of this approach by studying the cases of sodium and aluminum that crystallize in the bcc and fcc crystalline structures, respectively. Using these two generic collective variables, we perform variationally enhanced sampling and well tempered metadynamics simulations and find that the systems transform spontaneously and reversibly between the liquid and the solid phases. Discrete breathers dynamic in a model for DNA chain with a finite stacking enthalpy NASA Astrophysics Data System (ADS) Gninzanlong, Carlos Lawrence; Ndjomatchoua, Frank Thomas; Tchawoua, Clément 2018-04-01 The nonlinear dynamics of a homogeneous DNA chain based on site-dependent finite stacking and pairing enthalpies is studied. A new variant of extended discrete nonlinear Schrödinger equation describing the dynamics of modulated wave is derived. The regions of discrete modulational instability of plane carrier waves are studied, and it appears that these zones depend strongly on the phonon frequency of Fourier's mode. The staggered/unstaggered discrete breather (SDB/USDB) is obtained straightforwardly without the staggering transformation, and it is demonstrated that SDBs are less unstable than USDB. The instability of discrete multi-humped SDB/USDB solution does not depend on the number of peaks of the discrete breather (DB). By using the concept of Peierls-Nabarro energy barrier, it appears that the low-frequency DBs are more mobile. Determination of enthalpies of formation of energetic molecules with composite quantum chemical methods DOE PAGES Manaa, M. Riad; Fried, Laurence E.; Kuo, I-Feng W. 2016-02-01 We report gas-phase enthalpies of formation for the set of energetic molecules NTO, DADE, LLM-105, TNT, RDX, TATB, HMX, and PETN using the G2, G3, G4, and ccCA-PS3 quantum composite methods. Calculations for HMX and PETN hitherto represent the largest molecules attempted with these methods. G3 and G4 calculations are typically close to one another, with a larger difference found between these methods and ccCA-PS3. Furthermore there is significant uncertainty in experimental values, the mean absolute deviation between the average experimental value and calculations are 12, 6, 7, and 3 kcal/mol for G2, G3, G4, and ccCA-PS3, respectively. High enthalpy arc-heated plasma flow diagnostics by tunable diode laser absorption spectroscopy NASA Astrophysics Data System (ADS) Lin, Xin; Chen, Lianzhong; Zeng, Hui; Ou, Dongbin; Dong, Yonghui 2017-05-01 This paper reports the laser absorption measurements of atomic oxygen in the FD04 arc-heater at China Academy of Aerospace Aerodynamics (CAAA). An atomic oxygen absorption line at 777.19 nm is utilizied for detecting the population of electronically excited oxygen atom in an air plasma flow. A scanned-wavelength direct absorption mode is used in this study. The laser is scanned in wavelength across the absorption feature at a rate of 200 Hz. Under the assumption of thermal equilibrium, time-resolved temperature measurements are obtained on one line-of-sight in the arc-heater. The good agreement of the temperature inferred from the sonic throat method suggests the equilibrium assumption is valid. These results illustrate the feasibility of the diode laser sensors for flow parameters in high enthalpy arc-heated facilities. Altered Enthalpy-Entropy Compensation in Picomolar Transition State Analogues of Human Purine Nucleoside Phosphorylase† PubMed Central Edwards, Achelle A.; Mason, Jennifer M.; Clinch, Keith; Tyler, Peter C.; Evans, Gary B.; Schramm, Vern L. 2009-01-01 Human purine nucleoside phosphorylase (PNP) belongs to the trimeric class of PNPs and is essential for catabolism of deoxyguanosine. Genetic deficiency of PNP in humans causes a specific T-cell immune deficiency and transition state analogue inhibitors of PNP are in development for treatment of T-cell cancers and autoimmune disorders. Four generations of Immucillins have been developed, each of which contains inhibitors binding with picomolar affinity to human PNP. Full inhibition of PNP occurs upon binding to the first of three subunits and binding to subsequent sites occurs with negative cooperativity. In contrast, substrate analogue and product bind without cooperativity. Titrations of human PNP using isothermal calorimetery indicate that binding of a structurally rigid first-generation Immucillin (K d = 56 pM) is driven by large negative enthalpy values (ΔH = −21.2 kcal/mol) with a substantial entropic (-TΔS) penalty. The tightest-binding inhibitors (K d = 5 to 9 pM) have increased conformational flexibility. Despite their conformational freedom in solution, flexible inhibitors bind with high affinity because of reduced entropic penalties. Entropic penalties are proposed to arise from conformational freezing of the PNP·inhibitor complex with the entropy term dominated by protein dynamics. The conformationally flexible Immucillins reduce the system entropic penalty. Disrupting the ribosyl 5′-hydroxyl interaction of transition state analogues with PNP causes favorable entropy of binding. Tight binding of the seventeen Immucillins is characterized by large enthalpic contributions, emphasizing their similarity to the transition state. By introducing flexibility into the inhibitor structure, the enthalpy-entropy compensation pattern is altered to permit tighter binding. PMID:19425594 Enthalpy-Driven RNA Folding: Single-Molecule Thermodynamics of Tetraloop–Receptor Tertiary Interaction† PubMed Central Fiore, Julie L.; Kraemer, Benedikt; Koberling, Felix; Edmann, Rainer; Nesbitt, David J. 2010-01-01 RNA folding thermodynamics are crucial for structure prediction, which requires characterization of both enthalpic and entropic contributions of tertiary motifs to conformational stability. We explore the temperature dependence of RNA folding due to the ubiquitous GAAA tetraloop–receptor docking interaction, exploiting immobilized and freely diffusing single-molecule fluorescence resonance energy transfer (smFRET) methods. The equilibrium constant for intramolecular docking is obtained as a function of temperature (T = 21–47 °C), from which a van’t Hoff analysis yields the enthalpy (ΔH°) and entropy (ΔS°) of docking. Tetraloop–receptor docking is significantly exothermic and entropically unfavorable in 1 mM MgCl2 and 100 mM NaCl, with excellent agreement between immobilized (ΔH° = −17.4 ± 1.6 kcal/mol, and ΔS° = −56.2 ± 5.4 cal mol−1 K−1) and freely diffusing (ΔH° = −17.2 ± 1.6 kcal/mol, and ΔS° = −55.9 ± 5.2 cal mol−1 K−1) species. Kinetic heterogeneity in the tetraloop–receptor construct is unaffected over the temperature range investigated, indicating a large energy barrier for interconversion between the actively docking and nondocking subpopulations. Formation of the tetraloop–receptor interaction can account for ∼60% of the ΔH° and ΔS° of P4–P6 domain folding in the Tetrahymena ribozyme, suggesting that it may act as a thermodynamic clamp for the domain. Comparison of the isolated tetraloop–receptor and other tertiary folding thermodynamics supports a theme that enthalpy- versus entropy-driven folding is determined by the number of hydrogen bonding and base stacking interactions. PMID:19186984 The new insight into dynamic crossover in glass forming liquids from the apparent enthalpy analysis NASA Astrophysics Data System (ADS) Martinez-Garcia, Julio Cesar; Martinez-Garcia, Jorge; Rzoska, Sylwester J.; Hulliger, Jürg 2012-08-01 One of the most intriguing phenomena in glass forming systems is the dynamic crossover (TB), occurring well above the glass temperature (Tg). So far, it was estimated mainly from the linearized derivative analysis of the primary relaxation time τ(T) or viscosity η(T) experimental data, originally proposed by Stickel et al. [J. Chem. Phys. 104, 2043 (1996), 10.1063/1.470961; Stickel et al. J. Chem. Phys. 107, 1086 (1997)], 10.1063/1.474456. However, this formal procedure is based on the general validity of the Vogel-Fulcher-Tammann equation, which has been strongly questioned recently [T. Hecksher et al. Nature Phys. 4, 737 (2008), 10.1038/nphys1033; P. Lunkenheimer et al. Phys. Rev. E 81, 051504 (2010), 10.1103/PhysRevE.81.051504; J. C. Martinez-Garcia et al. J. Chem. Phys. 134, 024512 (2011)], 10.1063/1.3514589. We present a qualitatively new way to identify the dynamic crossover based on the apparent enthalpy space (H_a^' = {{dln τ}/{d(1/T)}}) analysis via a new plot ln H_a^' vs. 1/T supported by the Savitzky-Golay filtering procedure for getting an insight into the noise-distorted high order derivatives. It is shown that depending on the ratio between the "virtual" fragility in the high temperature dynamic domain (mhigh) and the "real" fragility at Tg (the low temperature dynamic domain, m = mlow) glass formers can be splitted into two groups related to f < 1 and f > 1, (f = mhigh/mlow). The link of this phenomenon to the ratio between the apparent enthalpy and activation energy as well as the behavior of the configurational entropy is indicated. Piezoelectric crystal microbalance measurements of enthalpy of sublimation of C2-C9 dicarboxylic acids NASA Astrophysics Data System (ADS) Dirri, F.; Palomba, E.; Longobardo, A.; Zampetti, E. 2016-02-01 We present here a novel experimental set-up that is able to measure the enthalpy of sublimation of a given compound by means of piezoelectric crystal microbalances (PCMs). The PCM sensors have already been used for space measurements, such as for the detection of organic and non-organic volatile species and refractory materials in planetary environments. In Earth atmospherics applications, PCMs can be also used to obtain some physical-chemical processes concerning the volatile organic compounds (VOCs) present in atmospheric environments. The experimental set-up has been developed and tested on dicarboxylic acids. In this work, a temperature-controlled effusion cell was used to sublimate VOC, creating a molecular flux that was collimated onto a cold PCM. The VOC recondensed onto the PCM quartz crystal, allowing the determination of the deposition rate. From the measurements of deposition rates, it has been possible to infer the enthalpy of sublimation of adipic acid, i.e. ΔHsub : 141.6 ± 0.8 kJ mol-1, succinic acid, i.e. 113.3 ± 1.3 kJ mol-1, oxalic acid, i.e. 62.5 ± 3.1 kJ mol-1, and azelaic acid, i.e. 124.2 ± 1.2 kJ mol-1. The results obtained show an accuracy of 1 % for succinic, adipic, and azelaic acid and within 5 % for oxalic acid and are in very good agreement with previous works (within 6 % for adipic, succinic, and oxalic acid and within 11 % or larger for azelaic acid). Piezoelectric crystal microbalance measurements of enthalpy of sublimation of C2-C9 dicarboxylic acids NASA Astrophysics Data System (ADS) Dirri, F.; Palomba, E.; Longobardo, A.; Zampetti, E. 2015-07-01 We present here a novel experimental setup able to measure the enthalpy of sublimation of a given compound by means of Piezoelectric Crystal Microbalances (PCM). This experiment was performed in the TG-Lab facility in IAPS-INAF, dedicated to the development of TGA sensors for space measurements, such as detection of organic and non-organic volatile species and refractory materials in planetary environments. In order to study physical-chemical processes concerning the Volatile Organic Compounds (VOC) present in atmospheric environments, the setup has been tested on Dicarboxylic acids. Acids with low molecular weight are among the components of organic fraction of particulate matter in the atmosphere, coming from different sources (biogenic and anthropogenic). Considering their relative abundance, it is useful to consider Dicarboxylic acid as "markers" to define the biogenic or anthropogenic origin of the aerosol, thus obtaining some information of the emission sources. In this work, a temperature controlled effusion cell was used to sublimate VOC, creating a molecular flux that was collimated onto a cold PCM. The VOC re-condensed onto the PCM quartz crystal allowing the determination of the deposition rate. From the measurements of deposition rates, it was possible to infer the enthalpy of sublimation of Adipic acid, i.e. Δ Hsub: 141.6 ± 0.8 kJ mol-1, Succinic acid, i.e. 113.3 ± 1.3 kJ mol-1, Oxalic acid, i.e. 62.5 ± 3.1 kJ mol-1 and Azelaic acid, i.e. 124.2 ± 1.2 kJ mol-1 (weight average values). The results obtained are in very good agreement with literature within 10 % for the Adipic, Succinic and Oxalic acid. Measuring Enthalpy of Sublimation of Volatiles by Means of Piezoelectric Crystal Microbalances NASA Astrophysics Data System (ADS) Dirri, Fabrizio; Palomba, Ernesto; Longobardo, Andrea; Zampetti, Emiliano 2017-12-01 Piezoelectric Crystal Microbalances (PCM's) are widely used to study the chemical processes involving volatile compounds in any environment, such as condensation process. Since PCM's are miniaturized sensor, they are very suitable for planetary in situ missions, where can be used to detect and to measure the mass amount of astrobiologically significant compounds, such as water and organics. This work focuses on the realization and testing of a new experimental setup, able to characterize volatiles which can be found in a planetary environment. In particular the enthalpy of sublimation of some dicarboxylic acids has been measured. The importance of dicarboxylic acids in planetology and astrobiology is due to the fact that they have been detected in carbonaceous chondritic material (e.g. Murchinson), among the most pristine material present in our Solar System. In this work, a sample of acid was heated in an effusion cell up to its sublimation. For a set of temperatures (from 30 °C to 75 °C), the deposition rate on the PCM surface has been measured. From these measurements, it has been possible to infer the enthalpy of sublimation of Adipic acid, i.e. ΔH = 141.6 ± 0.8 kJ/mol and Succinic acid, i.e. ΔH = 113.3 ± 1.3 kJ/mol. This technique has so demonstrated to be a good choice to recognise a single compound or a mixture (with an analysis upstream) even if some improvements concerning the thermal stabilization of the system will be implemented in order to enhance the results' accuracy. The experiment has been performed in support of the VISTA (Volatile In Situ Thermogravimetry Analyzer) project, which is included in the scientific payload of the ESA MarcoPolo-R mission study. Comparison of Maxillary Molar Distalization with an Implant-Supported Distal Jet and a Traditional Tooth-Supported Distal Jet Appliance PubMed Central Cozzani, Mauro; Pasini, Marco; Zallio, Francesco; Ritucci, Robert; Mutinelli, Sabrina; Mazzotta, Laura; Giuca, Maria Rita; Piras, Vincenzo 2014-01-01 Aim. To investigate and compare the efficiency of two appliances for molar distalization: the bone-anchored distal screw (DS) and the traditional tooth-supported distal jet (DJ) for molar distalization and anchorage loss. Methods. Tests (18 subjects) were treated with a DS and controls (18 subjects) were treated with a DJ. Lateral cephalograms were obtained before and at the end of molar distalization and were analysed. Shapiro Wilk test, unpaired t-test, and Wilcoxon rank-sum test were applied according to values distribution. The α level was fixed at 0.05. Results. Maxillary first molars were successfully distalized into a Class I relationship in all patients. The mean molar distalization and treatment time were similar in both groups. The DS group exhibited a spontaneous distalization (2.1 ± 0.9 mm) of the first premolar with control of anchorage loss, distal tipping, extrusion, and skeletal changes. Conclusions. The DS is an adequate compliance-free distalizing appliance that can be used safely for the correction of Class II malocclusions. In comparison to the traditional DJ, the DS enables not only a good rate of molar distalization, but also a spontaneous distalization of the first premolars. PMID:25018770 Endodontic treatment of a mandibular first molar with three mesial canals and broken instrument removal. PubMed Faramarzi, Farhad; Fakhri, Hamidreza; Fakri, Hamidreza; Javaheri, Homan H 2010-04-01 To succeed in any dental procedure, the clinician's awareness of the patient's dental anatomy and its variations is crucial. In endodontic therapy, obtaining full information about the root canals' variations can affect the outcome substantially. This case report presents the endodontic treatment of a mandibular first molar exhibiting three mesial root canals with 4 mm of a separated K-file in the coronal third of the mesiolingual canal on an 18-year-old female patient. This case demonstrates the importance of locating additional canals in any roots undergoing endodontic treatment and how the clinician's awareness of aberrant internal anatomy may change the treatment results. Unusual anatomy of a maxillary first molar with two palatal roots: a case report. PubMed Tomazinho, Flávia S F; Baratto-Filho, Flares; Zaitter, Suellen; Leonardi, Denise P; Gonzaga, Carla C 2010-03-01 The success of endodontic therapy is based on good endodontic access, correct cleaning and shaping, and adequate root canal obturation. However, endodontic treatment is also dependent on a sound knowledge of the internal anatomy of human teeth, especially when anatomical variations are present. Certain anatomical changes may be present to varying degrees, and it is important to report these to improve the understanding and expertise of endodontic specialists. With this aim in mind, this study reports an example of a maxillary first molar showing unusual anatomy (four roots and six root canals) and describes the endodontic treatment that was employed. Odontometric analysis of permanent maxillary first molar in gender determination. PubMed Shireen, Ayesha; Ara, Syeda Arshiya 2016-01-01 This study was conducted to assess the sex determination potential from mesiodistal (MD) and buccolingual (BL) dimensions of permanent maxillary first molar. The study was conducted in the Department of Oral Medicine and Radiology, Al-Badar Rural Dental College and Hospital, Gulbarga, Karnataka, on 600 subjects (300 male and 300 female), aged 17-25 years. The subjects were selected based on the inclusion and exclusion criteria set forth for the study. After obtaining informed consent, the intraoral measurements of MD and BL dimensions on casts of the first maxillary molars were taken using digital vernier caliper with resolution of 0.01 mm. The data obtained were subjected to statistical analysis using paired and unpaired t -test to compare MD and BL dimensions between males and females. P ≤0.05 was considered statistically significant. The mean MD width of the first maxillary molar was 10.60 ± 0.6644 mm (right) and 10.60 ± 0.6644 mm (left) in males and 10.40 ± 0.6255 mm (right) and 10.40 ± 0.6255 mm (left) in females. The mean BL width of the first maxillary molar was 11.60 ± 1.2227 mm (right) and 11.60 ± 1.2227 mm (left) in males and 11.20 ± 0.8440 mm (right) and 11.20 ± 0.8440 mm (left) in females. The differences between males and females in MD and BL dimensions measured were statistically significant (P < 0.05). Right and left MD dimensions exhibited sexual dimorphism of 1.92% and right and left BL dimensions exhibited sexual dimorphism of 3.57%. The MD and BL dimensions of the maxillary first molars may be used as an aid in sex discrimination. Impaction of permanent mandibular second molar: A retrospective study PubMed Central Altieri, Federica; Di Mambro, Alfonso; Galluccio, Gabriella; Barbato, Ersilia 2013-01-01 Objective: To determine the prevalence of impacted mandibular second molar (MM2) and the association between MM2 impaction and crowding. The clinical significance of the angle between first and second mandibular molar and of the space between the first mandibular molar (MM1) and the anterior margin of mandibular ramus in MM2 impaction were also evaluated. Material and Methods: In this retrospective study , from the dental records of 2,945 caucasian young orthodontics patients, 40 subjects with MM2 impaction were included in a study group (SG) and compared with a control group (CG) of 200 subjects without MM2 impactions. The crowding, the angle of inclination of MM2, the distance between MM1 and mandibular ramus, the canine and molar relationships, and the lower centre line discrepancy were measured. For the statistical analysis , descriptive statistics and t-Student for independent sample groups were used. Results: The prevalence of impacted MM2 was 1.36%. The independent-Samples t-Test between SG and CG showed: the presence of crowding (P≤0.001), an higher angle values of MM2 inclination (P≤0.001) and a smaller distance between MM1 and the anterior margin of mandibular ramus (P≤0.001) in the SG. Conclusion: The impaction of MM2 is a relatively rare occurrence in orthodontic caucasian populations. The crowding, a higher angle values of MM2 inclination and a reduced distance between MM1 and the anterior margin of mandibular ramus, at the time of one third of MM2 root formation (T1), characterize MM2 impaction. Key words:Impacted mandibular second molar, impaction, orthodontics. PMID:23524438 The radix entomolaris in mandibular first molars: an endodontic challenge. PubMed De Moor, R J G; Deroose, C A J G; Calberson, F L G 2004-11-01 To present cases of mandibular first molars with an additional distolingual root (radix entomolaris, RE) and to survey the literature on the incidence of this anatomical feature. A major anatomical variant of the two-rooted mandibular first molar is a tooth with an additional distolingual and third root: the RE. The prevalence of these three-rooted mandibular first molars appears to be less than 3% in African populations, not to exceed 4.2% in Caucasians, to be less than 5% in Eurasian and Asian populations, and to be higher than 5% (even up to 40%) in populations with Mongolian traits. A total of 18 cases (12 root filled and six extracted mandibular first molars) with an RE were collected during the years 2000-2003 in patients of Caucasian origin. As far as the access was concerned, entering the root canal in the RE required a modification of the opening in a distolingual direction resulting in a trapezoidal opening cavity. None of the orifices was located midway between the mesial and distal root component. Based on the anatomy of the extracted samples and the bending of ISO 10 files after scouting of the root canal in the RE, three types of curvature were detected: (I) straight or no curvature (two cases); (II) coronal third curved and straight continuation to the apex (five cases); and (III) curvature in the coronal third and buccal curvature from the middle third or apical third of the root (11 cases). Clinicians should be aware of this unusual root morphology in mandibular first molars in Caucasian people. Radiographs exposed at two different horizontal angles are needed to identify this additional root. The access cavity must be modified in a distolingual direction in order to visualize and treat the RE, this results in a trapezoidal access cavity. Localization of type IV collagen a 1 to a 6 chains in basement membrane during mouse molar germ development. PubMed Nagai, N; Nakano, K; Sado, Y; Naito, I; Gunduz, M; Tsujigiwa, H; Nagatsuka, H; Ninomiya, Y; Siar, C H 2001-10-01 The dental basement membrane (BM) putatively mediates epithelial-mesenchymal interactions during tooth morphogenesis and cytodifferentiation. Type IV collagen alpha chains, a major network-forming protein of the dental BM, was studied and results disclosed distinct expression patterns at different stages of mouse molar germ development. At the dental placode and bud stage, the BM of the oral epithelium expressed alpha 1, alpha 2, alpha 5 and alpha 6 chains while the gubernaculum dentis, in addition to the above four chains, also expressed a 4 chain. An asymmetrical expression for alpha 4, alpha 5 and alpha 6 chains was observed at the bud stage. At the early bell stage, the BM associated with the inner enamel epithelium (IEE) of molar germ expressed alpha 1, alpha 2 and alpha 4 chains while the BM of the outer enamel epithelium (OEE) expressed only alpha 1 and a 2 chains. With the onset of dentinogenesis, the collagen a chain profile of the IEE BM gradually disappeared. Howeverfrom the early to late bell stage, the gubernaculum dentis consistently expressed alpha 1, alpha 2, alpha 5 and a 6 chains resembling fetal oral mucosa. These findings suggest that stage- and position-specific distribution of type IV collagen alpha subunits occur during molar germ development and that these changes are essential for molar morphogenesis and cytodifferentiation. Characterization of branched ultrahigh molar mass polymers by asymmetrical flow field-flow fractionation and size exclusion chromatography. PubMed Otte, T; Pasch, H; Macko, T; Brüll, R; Stadler, F J; Kaschta, J; Becker, F; Buback, M 2011-07-08 narrow distributed polystyrene standards as reference materials with known structure by AT/HT-SEC and AT/HT-AF4. Low density polyethylenes as well as polypropylene and polybutadiene, containing high degrees of branching and high molar masses, have been analyzed with both methods. As in SEC the relationship between the radius of gyration (R(g)) or the molar mass and the elution volume is curved up towards high elution volumes, a correct calculation of the MMD and the molar mass average or branching ratio is not possible using the data from the SEC measurements. In contrast to SEC, AF4 allows the precise determination of the MMD, the molar mass averages as well as the degree of branching because the molar mass vs. elution volume curve and the conformation plot is not falsified in this technique. In addition, higher molar masses can be detected using HT-AF4 due to the absence of significant shear degradation in the channel. As a result the average molar masses obtained from AF4 are higher compared to SEC. The analysis time in AF4 is comparable to that of SEC but the adjustable cross-flow program allows the user to influence the separation efficiency which is not possible in SEC without a costly change of the whole column combination. Copyright © 2011 Elsevier B.V. All rights reserved. Standardized method to produce tetracycline-stained human molar teeth in vitro. PubMed Chan, Daniel C N; Rozier, Gregory Shayne; Steen, Angela; Browning, William D; Mozaffari, Mahmood S 2006-09-01 This study tested the hypothesis that exposure of human molar teeth to tetracycline (TCN) derivatives in vitro results in tooth discoloration resembling the clinical presentation of TCN staining. The effects of exposure of 20 extracted human molar teeth to distilled water, chlortetracycline, doxycycline, or minocycline were compared. The baseline color of each tooth was analyzed with a dental spectrophotometer. The pulp chambers were each filled with a TCN derivative solution and then sealed. The teeth were placed in a centrifuge tube and then centrifuged at 2800 rpm for 20 minutes. Color change was monitored weekly for 7 weeks. Digital images of the surfaces were recorded. For each specimen at every evaluation period, color change from baseline was calculated using Commission Internationale d'Eclairage (CIE) Delta E 2000 (deltae00). There was a significant association between the type of derivative used and deltae00, as well as between the evaluation period and deltae00. There was also a significant association between the interaction term, derivative x evaluation period, and deltae00. Results of the Holm-Sidak post hoc test demonstrated that all 3 TCN derivatives were associated with significantly larger deltae00 than the control group (P < or = .05). All 3 TCN derivative solutions produced significant color changes as time progressed. Different TCN derivatives produced a different L* (lightness), C* (chroma), and H* (hue), with minocycline behaving distinctly differently from chlortetracycline and doxycycline. The model could be used to study the underlying mechanisms of TCN staining as well as many aspects of vital tooth